
EARLY RISK STRATIFICATION OF DOSING ERRORS IN CLINICAL TRIALS USING MACHINE LEARNING

A PREPRINT

 **Félicien Hêche***

Department of Radiology and Medical Informatics
University of Geneva
Geneva, Switzerland
felicien.heche@unige.ch

 **Sohrab Ferdowsi***

Department of Radiology and Medical Informatics
University of Geneva
Geneva, Switzerland
sohrab.ferdowsi@unige.ch

 **Anthony Yazdani**

Department of Radiology and Medical Informatics
University of Geneva
Geneva, Switzerland
anthony.yazdani@unige.ch

Sara Sansaloni-Pastor

Actelion Pharmaceuticals Ltd
Basel, Switzerland
SSansalo@ITS.JNJ.com

 **Douglas Teodoro**

Department of Radiology and Medical Informatics
University of Geneva
Geneva, Switzerland
douglas.teodoro@unige.ch

February 27, 2026

ABSTRACT

Objective: The objective of this study is to develop a machine learning (ML)-based framework for early risk stratification of clinical trials (CTs) according to their likelihood of exhibiting a high rate of dosing errors, using information available prior to trial initiation.

Materials and Methods: We constructed a dataset from ClinicalTrials.gov comprising 42,112 CTs. Structured, semi-structured trial data, and unstructured protocol-related free-text data were extracted. CTs were assigned binary labels indicating elevated dosing error rate, derived from adverse event reports, MedDRA terminology, and Wilson confidence intervals. We evaluated an XGBoost model trained on structured features, a ClinicalModernBERT model using textual data, and a simple late-fusion model combining both modalities. Post-hoc probability calibration was applied to enable interpretable, trial-level risk stratification.

Results: The late-fusion model achieved the highest AUC-ROC (0.862). Beyond discrimination, calibrated outputs enabled robust stratification of CTs into predefined risk categories. The proportion of trials labeled as having an excessively high dosing error rate increased monotonically across higher predicted risk groups and aligned with the corresponding predicted probability ranges.

Discussion: These findings indicate that dosing error risk can be anticipated at the trial level using pre-initiation information. Probability calibration was essential for translating model outputs into reliable and interpretable risk categories, while simple multimodal integration yielded performance gains without requiring complex architectures.

Conclusion: This study introduces a reproducible and scalable ML framework for early, trial-level risk stratification of CTs at risk of high dosing error rates, supporting proactive, risk-based quality management in clinical research.

*These authors contributed equally to this work.

Keywords Machine learning · Medication errors · Clinical trials · Risk stratification · Medical NLP

1 Introduction

Medication errors, defined as failures in the treatment process that lead to, or have the potential to lead to, harm to the patient [1], constitute a significant threat to public health worldwide. Despite sustained efforts to improve medication safety, these events continue to impose a substantial burden on healthcare systems [2, 3, 4]. In response, major health authorities have prioritized medication safety as a core component of patient safety strategies. Notably, the World Health Organization (WHO) launched the Medication Without Harm initiative to catalyze coordinated action aimed at reducing severe, avoidable medication-related harm [5], and has since reinforced this commitment through targeted policy guidance [6].

In parallel with these policy-driven efforts, machine learning (ML) approaches have been increasingly adopted in healthcare to support tasks such as medical image interpretation [7, 8], early detection of disease [9, 10], personalized treatment planning [11, 12], and the assessment of operational risks in clinical trials (CTs) [13, 14, 15]. A key strength of ML lies in its ability to model high-dimensional, heterogeneous, and often multimodal data [16, 17], enabling the discovery of complex associations between patient characteristics, treatments, and outcomes that may elude conventional analytic approaches [18, 19]. When appropriately integrated into clinical and research workflows, such models can support timely decision-making and contribute to improved medication safety [20, 21].

Despite these advances, important limitations remain in the application of ML to medication error detection. Specifically, as highlighted in a recent scoping review [22], existing ML-based studies focus almost exclusively on errors occurring during routine clinical care. Notably, this review identified no prior work addressing medication errors arising in research and development settings. This gap is surprising given the importance of the pharmaceutical research sector, which involves annual global investments exceeding US \$250 billion [23], as well as the potential consequences of such errors. Indeed, medication errors in CTs can compromise trial validity and data integrity [24], jeopardize participant safety [25], and lead to regulatory non-compliance [26]. These reasons, among other factors for the failure of trials, result in an overall success rate of no more than 14% for trials making it from phase I to the final market approval [27], prolonging the average 13.8-year-long drug development cycle [28], as well as contributing to the average 1.3B\$ of drug development [29].

In this study, we introduce an ML framework for early risk stratification of clinical trials (CTs) according to their likelihood of exhibiting a high rate of dosing errors, using information available prior to trial initiation. The proposed approach relies on data extracted from ClinicalTrials.gov, a large, publicly accessible registry of CTs maintained by the U.S. National Library of Medicine. This resource provides detailed protocol-level information, including eligibility criteria, and study design characteristics, alongside standardized adverse event reporting. Reporting to ClinicalTrials.gov is subject to statutory requirements for interventional drug trials, supporting the reliability and consistency of the reported data. This unique combination of scale, structure, and regulatory grounding makes this resource particularly well suited for large-scale, multimodal ML analyses of trial-level dosing error risk.

Our contributions are the following. First, we propose a multimodal ML framework for early, trial-level risk stratification of CTs according to their likelihood of exhibiting elevated dosing error rates. This approach integrates structured and semi-structured CT data and unstructured protocol-level text to support calibrated, trial-level stratification into actionable risk categories. Second, we publicly release the dataset used in this study, augmented with curated features and outcome labels, on Hugging Face. By making this resource openly available, we aim to facilitate reproducible research and stimulate further methodological development at the intersection of ML and CT safety. Finally, we provide the complete codebase used to construct the dataset and implement the proposed models on GitHub. Particular emphasis was placed on reproducibility. We introduce a pipeline that enables automated ingestion of protocols with carefully designed data structures that capture the hierarchical nature of the CTGov’s data fields, as well as strict validation of entries during parsing. This makes the reconstruction and extension of the dataset from the raw instances of ClinicalTrials.gov registry fully automated and reproducible.

This paper is organized as follows. Section 2 details the dataset construction process and the proposed ML methodology. Section 3 presents the experimental results. Section 4 interprets these findings and discusses their implications for CT safety and quality management. Section 5 concludes the paper.

2 Materials and Methods

Figure 1 provides an overview of the dataset construction pipeline. Relevant CTs are first selected according to predefined inclusion criteria, as detailed in Section 2.1, notably to ensure the availability of dosing-related information.

Information available prior to trial initiation is then extracted and ingested using customized data structures, from which predictive features are derived (Section 2.2). The procedure used to assign dosing error–related risk labels is described in Section 2.3.

The resulting dataset is subsequently partitioned into training, validation, and test sets using a chronological splitting strategy (Section 2.4). We then present the ML models and their evaluation procedures in Section 2.5, followed by the trial-level risk assessment framework in Section 2.6.

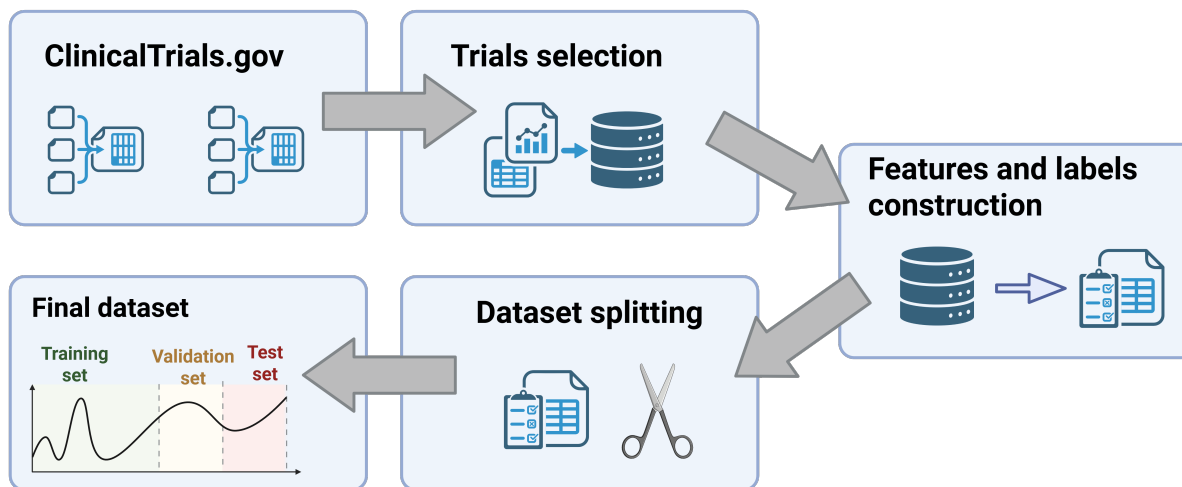


Figure 1: Overview of the dataset construction steps, from CTs selection to feature and label construction and dataset splitting. Created with BioRender.

2.1 Trials selection

The ClinicalTrials.gov registry was used as the primary source of clinical studies data, from which we construct our dataset. All CTs meeting the following inclusion criteria were retrieved: (i) completed or terminated trial status; (ii) interventional study design; (iii) availability of study results; (iv) a reported completion date; and (v) registration prior to a fixed cut-off date of September 1, 2025. In total, 42,112 CTs satisfied these criteria and were included in the dataset.

Restricting the dataset to completed or terminated trials guarantees that all included studies have concluded, while limiting the cohort to interventional designs focuses the analysis on therapeutic trials and excludes observational studies. Requiring available results ensures access to reported outcomes, such as adverse events. The availability of a completion date supports the temporal splitting strategy described in Section 2.4. Finally, the use of a fixed cut-off date ensures reproducibility.

2.2 Data extraction and feature creation

All information fields available on ClinicalTrials.gov were screened to identify a relevant set of features. To reflect a realistic deployment scenario and avoid temporal leakage, only information available prior to trial initiation was retained as predictive input. To ensure data reliability and consistency, structured features were extracted using data validation tools such as the Pydantic library [30], or Python’s standard data types, such as the enumerated data structures (Enum) [31], which constrain categorical variables to predefined value sets and prevent invalid or inconsistent entries. These schemas were created according to the structures defined in CTGov’s instructions.

The resulting feature set comprises categorical, numerical, and textual variables. An overview of these features is provided in Tables 1. Mappings between categorical encodings and their semantic meanings are provided in Appendix A.

In addition to the predictive features and labels used in the present study, we extracted a set of auxiliary information to support flexible reuse of the dataset beyond its primary objective. These elements are intended to enable future investigations at the intersection of ML and CT safety, such as the construction of alternative datasets, analyses of trial design characteristics, or exploratory studies of discrepancies between enrollment and exposure populations. A description of this additional information is provided in Appendix B.

Categorical and binary features				
Feature name	Data type	Missing (%)	Most frequent class (%)	Description
primaryPurpose	Categorical	0.94	Treatment (84)	Primary objective of the study
	masking	Categorical	0.18	None (52)
sex	Categorical	0.02	All (88)	Sex eligibility criteria for participants
phases	Categorical (multi-label)	0.01	Phase II (41)	Clinical development phase(s) of the trial
armGroupTypes	Categorical (multi-label)	0.60	Experimental (64)	Type(s) of study arms
interventionTypes	Categorical (multi-label)	0.00	Drug (87)	Category(ies) of interventions evaluated
healthyVolunteers	Binary	0.06	False (86)	Eligibility of healthy volunteers for enrollment
oversightHasDmc	Binary	12.00	False (53)	Presence of a data monitoring committee
Numeric features				
Feature name	Data type	Missing (%)	Mean (SD)	Description
enrollmentCount	Numeric (count)	0.00	264 (4,810)	Number of enrolled participants
numArms	Numeric (count)	0.00	2.33 (1.71)	Number of study arms per trial
numInterventions	Numeric (count)	0.00	2.48 (1.68)	Number of distinct interventions evaluated
numLocations	Numeric (count)	0.00	22.9 (62.9)	Number of trial sites or locations
Text features				
Feature name	Data type	Missing (%)	Mean characters (SD)	Description
allocation	Free text	0.38	8.46 (3.92)	Allocation method used to assign participants to study arms
interventionModel	Free text	0.33	9.34 (1.78)	Intervention assignment model
briefSummary	Free text	0.00	502.40 (464.74)	Short textual summary of the trial
detailedDescription	Free text	38.00	1610.83 (1676.93)	Detailed description of objectives, design, and procedures
conditions	Free text	0.00	39.21 (120.66)	Medical condition(s) studied
conditionsKeywords	Free text	36.00	81.17 (155.22)	Additional condition-related keywords
armDescriptions	Free text	0.60	388.24 (553.24)	Free-text descriptions of study arms
interventionNames	Free text	0.00	82.72 (65.33)	Names of interventions reported in the trial
interventionDescriptions	Free text	0.00	286.18 (340.14)	Descriptions of the interventions evaluated
locationDetails	Free text	5.60	1310.26 (3512.07)	Textual information describing trial locations

Table 1: Overview of categorical/binary, numeric, and text features extracted from ClinicalTrials.gov. For each feature type, we report the corresponding summary statistic: most frequent class for categorical/binary variables, mean (SD) for numeric variables, and mean character length (SD) for text fields.

2.3 Label assignment

Dosing errors were identified using the standardized adverse event reporting framework of ClinicalTrials.gov, which relies on terminology from the Medical Dictionary for Regulatory Activities (MedDRA version 27.1, English) [32]. MedDRA terms are organized hierarchically from general to more specific. Within this hierarchy, two High-Level Group Terms (HLGTs) related to dosing errors (*10079145: "Overdoses and underdoses NEC"* and *10079159: "Medication errors and other product use errors and issues"*) were selected. All the 630 descendants of these two nodes

corresponding to the lower levels of the hierarchy, i.e., the High-Level Terms (HLTs), the Preferred Terms (PTs) and the Low-Level Terms (LLTs) were independently reviewed by a team of clinical pharmacology experts to focus only on the dosing-related events. This resulted in 210 concepts that we matched against the reported Adverse Events (AEs) of the included CT protocols using Fuzzy matching and canonicalized to 81 concepts.

For each trial, the reported CT’s AEs were examined per Arm group, where we aggregated the number of participants at risk of experiencing adverse dosing events, as well as the actual occurring error numbers to the CT level and calculated dosing-error rates. Note that the number of participants may differ from the total number of enrolled participants, for example due to withdrawal prior to exposure.

Finally, a trial was labeled as positive if the lower bound of the 95% Wilson confidence interval for the dosing error rate exceeded a fixed threshold. Given the rare nature of dosing errors in clinical research and the pharmacovigilance practice of treating very low-frequency events as meaningful safety signals [33], a low operational threshold of 0.01% was adopted. Using this criterion, 4.62% of the CTs in the dataset were labeled as positive, i.e., indicating an unusually high rate of dosing errors. The complete labeling workflow, including MedDRA term selection, expert curation, adverse event matching, and statistical thresholding, is summarized in Figure 2.

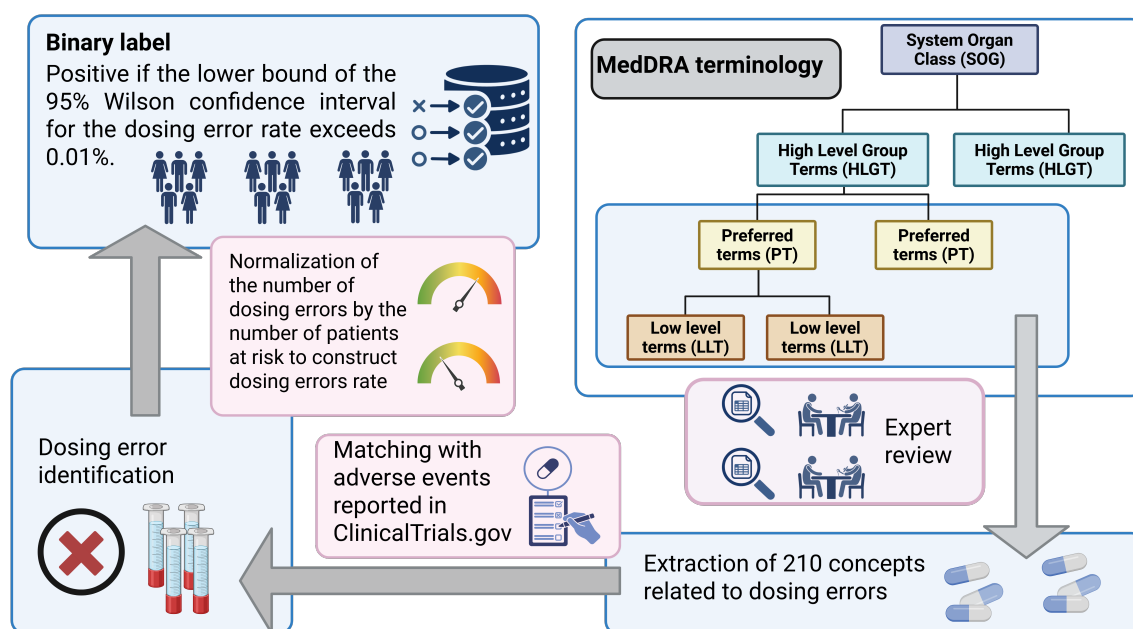


Figure 2: Overview of the dosing-error labeling pipeline. MedDRA high-level group terms were selected and reviewed by clinical pharmacology experts, matched to reported adverse events, aggregated at the trial level, and converted into binary risk labels using a Wilson confidence interval–based threshold. Created with BioRender

2.4 Dataset splitting strategy

A common practice when working with time-ordered data is to split observations chronologically and evaluate ML models on the most recent portion of the data, thereby providing a realistic estimate of prospective performance. Following this principle, we initially considered splitting the dataset based on trial initiation dates using a 70/15/15 train/validation/test split.

However, because the proposed pipeline relies exclusively on completed or terminated CTs, this strategy introduces a duration-dependent selection bias. As illustrated in Figure 3, for trials initiated later in the study period, only those with sufficiently short durations are available in the dataset, as longer trials initiated during the same period have not yet completed or terminated. Consequently, trials with shorter durations, and by extension, smaller enrollment sizes, are overrepresented in the validation and test sets.

To mitigate this bias, we instead sorted trials according to their completion dates prior to splitting. As shown in Figure 4, this approach reduces distributional shifts between the training, validation, and test sets.

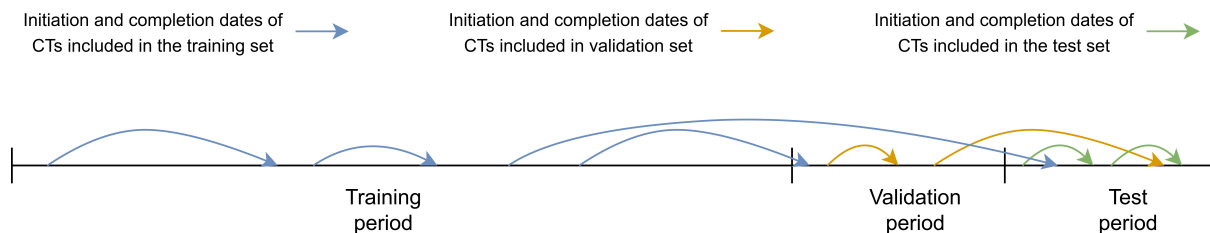


Figure 3: Illustration of the bias introduced by splitting CTs chronologically according to initiation dates. Because only completed or terminated trials are included, trials with shorter durations are more likely to fall within later time windows, leading to their overrepresentation in the validation and test sets.

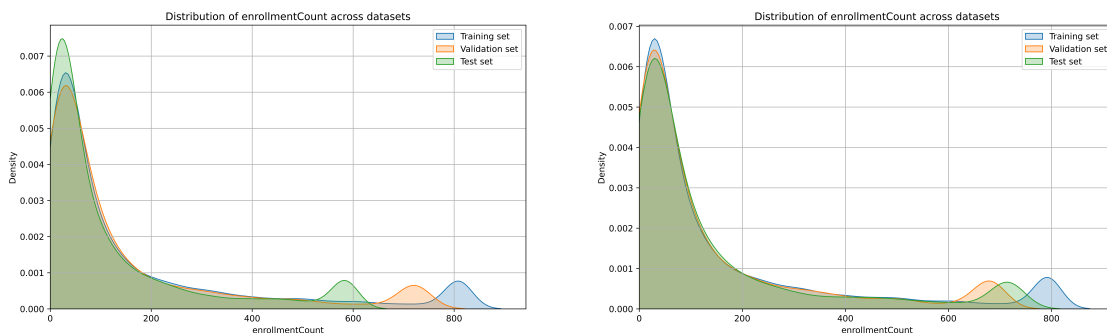


Figure 4: Comparison of distributional shifts induced by different temporal splitting strategies. Kernel density estimates of enrollment counts across the training, validation, and test sets are shown for each strategy; distributions are truncated at the 95th percentile for visualization purposes. The left panel shows splitting by trial initiation date, and the right panel shows splitting by trial completion date, which we adopt in this work.

2.5 Machine learning models

Our curated dataset contains fields with numerical, categorical, list-of-categoricals, and textual fields, where the latter may contain short textual descriptions with medical terminology. Our aim here is to establish a basic but robust baseline incorporating this multimodal information into the well-established predictive ML models.

Several standard ML models were trained and evaluated to assess their ability to identify CTs at risk of exhibiting a high dosing error rate. In addition to assessing predictive performance, these experiments were designed to examine whether different data modalities capture distinct and potentially complementary risk signals.

An XGBoost model [34] was trained using categorical and numerical features. A ClinicalModernBERT model [35] was fine-tuned using only the text features. Finally, a simple multimodal approach, referred to as LateFusion model, was evaluated by combining the predicted probabilities of the two unimodal models using a weighted average, with weights optimized on the validation set. Details regarding training and hyperparameter optimization are provided in Appendix C.

Model performance was primarily assessed using the area under the Receiver Operating Characteristic curve (AUC-ROC) to evaluate discrimination capacity. Additional metrics, including precision, recall, accuracy, and F1-score, were reported to provide a more comprehensive characterization of performance. Balanced accuracy and macro-averaged F1-score were computed to account for class imbalance. For metrics requiring a binary decision, the classification threshold was selected on the validation set to maximize the F1-score and then fixed for evaluation on the test set. Finally, the Brier score [36] was used to assess the accuracy of predicted probabilities, providing a calibration-sensitive measure of probabilistic performance.

2.6 Risk assessment

In this study, we move beyond binary trial classification and focus on trial-level risk assessment for dosing errors. Rather than determining whether a CT will exhibit an elevated incidence of dosing errors, the objective is to provide a principled and interpretable framework for quantifying and stratifying risk across trials.

Model	AUC	Brier	F1	F1 (macro)	Rec	Prec	BalAcc	Acc
XGBoost (uncal.)	0.848	0.105	0.293	0.619	0.423	0.224	0.674	0.900
XGBoost	0.848	0.042	0.292	0.619	0.423	0.222	0.674	0.899
ClinicalModernBERT (uncal.)	0.855	0.092	0.304	0.626	0.429	0.235	0.678	0.903
ClinicalModernBERT	0.855	0.042	0.306	0.628	0.426	0.239	0.678	0.905
LateFusion (uncal.)	0.862	0.090	0.300	0.633	0.284	0.318	0.626	0.935
LateFusion	0.862	0.041	0.298	0.632	0.281	0.319	0.625	0.935

Table 2: Classification performance on the test set before and after probability calibration. Best performance per metric is shown in bold.

This shift from classification to risk estimation places strong requirements on the reliability of predicted probabilities. A naïve interpretation of ML model outputs as direct estimates of dosing error risk is inappropriate, as it is well established that ML models produce poorly calibrated probability estimates [37, 38]. Raw model outputs cannot be reliably interpreted as absolute risk estimates and may substantially misrepresent true risk levels.

To address this limitation, we applied post-hoc probability calibration prior to downstream risk assessment. Calibrated probabilities were obtained using Platt scaling [39] for the ClinicalModernBERT and LateFusion models, and isotonic regression [40] for the XGBoost model. Calibration parameters were estimated exclusively on the validation set and subsequently applied unchanged to the test set.

The calibrated predicted probabilities were then used to stratify CTs into discrete risk categories reflecting their likelihood of exhibiting a high incidence of dosing errors. In the full dataset, approximately 4.6% of trials were classified as risky, providing an empirical estimate of the average baseline risk. Risk thresholds were therefore defined a priori to correspond to increasing multiples of this baseline, enabling a direct and intuitive interpretation of risk levels.

Specifically, the categories were constructed based on the predicted probability \hat{p} as follows:

- **Low risk:** $\hat{p} < 2\%$ (less than $0.5\times$ the average risk),
- **Moderate risk:** $2\% \leq \hat{p} < 5\%$ (approximately $0.5\text{--}1\times$ the average risk),
- **High risk:** $5\% \leq \hat{p} < 10\%$ (approximately $1\text{--}2\times$ the average risk),
- **Very high risk:** $\hat{p} \geq 10\%$ (greater than $2\times$ the average risk).

To evaluate the practical utility of the proposed risk categories, we report, for each model and each risk group, the number of assigned trials, the number of trials classified as problematic, the observed event rate, and the corresponding risk increase relative to the overall rate observed in the test set.

To further assess the robustness of the proposed risk stratification framework, we performed subgroup analyses across trial characteristics. Specifically, predicted risk groups were examined according to clinical development stage and enrollment size. Development stage was determined from the highest reported trial phase and mapped into three categories (early: Early Phase I or Phase I; mid: Phase II; late: Phase III or beyond). Enrollment size was grouped into predefined bins (≤ 50 , 51–200, 201–500, and > 500 participants). Within each subgroup and predicted risk category, we computed the number of trials, the number of problematic trials, the observed event rate, and the relative risk relative to the subgroup-specific baseline prevalence.

3 Results

Table 2 reports test-set classification performance for the evaluated ML models, including both uncalibrated and calibrated variants. Among the unimodal approaches, XGBoost obtained an AUC-ROC of 0.848, while ClinicalModernBERT achieved an AUC-ROC of 0.855. The LateFusion model yielded the highest AUC-ROC (0.862).

Across all evaluated models, post-hoc probability calibration substantially improved probabilistic accuracy, reducing Brier scores from approximately 0.09–0.11 to 0.04–0.05. As expected, calibration did not materially affect discriminative performance, with AUC-ROC values remaining unchanged.

Given that the calibrated LateFusion model achieved both the highest discriminative performance and the lowest Brier score among the evaluated approaches, we focus on this model for downstream risk stratification. Table 3 summarizes

Risk group	Number of CTs	Number of events	Event rate (%)	Relative risk
LateFusion (uncal.)				
Low	401	0	0.00	0.000
Moderate	1773	6	0.34	0.069
High	953	8	0.84	0.171
Very high	3191	296	9.28	1.89
LateFusion				
Low	3547	22	0.62	0.126
Moderate	948	26	2.74	0.559
High	738	58	7.86	1.602
Very high	1085	204	18.80	3.832

Table 3: Risk stratification of CTs on the test set using calibrated LateFusion predictions. Events correspond to trials labeled as exhibiting an elevated dosing error rate. Relative risks are reported relative to the overall event prevalence in the test set (4.91%).

the distribution of CTs across predicted risk groups on the test set, together with observed event rates and relative risks. Results for the remaining models are reported in the Appendix D.

Notably, the results obtained with the calibrated LateFusion model demonstrate a clear alignment between predefined risk categories and observed outcomes. Among CTs classified as low risk ($\hat{p} < 2\%$), 0.62% were labeled as problematic. This proportion increases to 2.74% for trials in the moderate-risk group ($2\% \leq \hat{p} < 5\%$), 7.86% in the high-risk group ($5\% \leq \hat{p} < 10\%$), and 18.80% in the very high-risk group ($\hat{p} \geq 10\%$). In addition, the proposed stratification distributes CTs across all predefined risk categories, avoiding collapse into a single dominant class and yielding non-degenerate risk groups. In contrast, risk stratification based on uncalibrated model outputs resulted in a markedly less informative allocation of trials across risk groups.

Subgroup analyses across development stage and enrollment size revealed consistent and informative patterns. As shown in Table 4, the monotonic increase in observed event rates across risk categories derived from the calibrated LateFusion model was preserved within early-, mid-, and late-stage trials. Within each development stage, event rates increased stepwise from the low- to the very high-risk groups defined by the model’s predicted probabilities, and the corresponding relative risks exhibited comparable monotonic increases. These findings indicate that risk categories maintain their discriminatory structure independently of clinical phase. Complementary analyses stratified by enrollment size (Appendix E) demonstrated a similar progressive enrichment of problematic trials across higher risk groups.

4 Discussion

These results suggest that dosing error risk in CTs can be anticipated using information that is available prior to trial initiation. By relying exclusively on CT design characteristics and protocol-related textual information, the proposed framework indicates that aspects of dosing error risk are associated with upstream design and planning decisions, supporting a preventive perspective on medication safety in clinical research.

Across models, multimodal integration of structured trial features and unstructured protocol text outperformed unimodal baselines. Notably, these improvements were achieved using a simple late-fusion strategy, without relying on complex multimodal architectures. This suggests that structured trial information and free-text protocol descriptions capture distinct and complementary aspects of dosing error risk, and that their integration can improve trial-level risk estimation.

Beyond discriminative performance, a key methodological insight concerns the role of probability calibration in enabling reliable and interpretable risk stratification. Models incorporating calibrated outputs yielded a partition of CTs into distinct risk categories, avoiding collapse into a single dominant class and exhibiting a clear, monotonic relationship between predicted risk levels and observed CTs with unusually high dosing error rates. In contrast, stratification based on uncalibrated model outputs resulted in substantially less informative groupings.

In addition, the subgroup analyses further support the structural robustness of the proposed framework. The preservation of monotonic risk trends within development phases and across enrollment categories suggests that the observed stratification cannot be reduced to simple proxies such as clinical stage or trial size. Rather, the model appears to capture more granular design-level characteristics that contribute to dosing error risk beyond these structural attributes.

Risk group	Number of CTs	Number of events	Event rate (%)	Relative risk
Early stage				
Low	642	3	0.47	0.235
Moderate	75	1	1.33	0.672
High	50	5	10.00	5.038
Very high	39	7	17.95	9.042
Mid stage				
Low	1853	14	0.76	0.201
Moderate	526	15	2.85	0.758
High	352	32	9.09	2.417
Very high	326	54	16.56	4.403
Late stage				
Low	934	5	0.54	0.070
Moderate	344	10	2.91	0.379
High	335	21	6.27	0.817
Very high	719	143	19.89	2.591

Table 4: Risk stratification by clinical development stage on the test set using calibrated LateFusion predictions. Relative risks are reported with respect to the prevalence within each development stage.

4.1 Implications for clinical trial quality management

The ability to anticipate dosing error risk using information available prior to trial initiation has direct implications for CT quality management. By providing an interpretable, trial-level risk signal early in the study lifecycle, the proposed framework enables a more proactive and proportionate approach to risk mitigation. Notably, the preservation of risk enrichment patterns across development phases and enrollment sizes suggests that the approach remains informative across heterogeneous clinical contexts, including trials at different stages of development and of varying scale. Rather than applying uniform review processes across all trials, risk stratification therefore allows preventive efforts to be tailored according to the estimated likelihood of dosing-related issues, independent of trial phase or size.

The proposed framework could be integrated into existing CT review and governance workflows as a decision-support tool during the planning phase. Predicted risk categories provide a quantitative and interpretable signal that can complement established review criteria. In practice, this information may inform targeted protocol refinements, particularly with respect to dosing schedules, administration procedures, or monitoring plans, or motivate the implementation of additional safeguards prior to trial initiation. Importantly, the framework is not intended to replace expert judgment, but rather to augment it by providing a data-driven risk signal that is available early in the trial lifecycle.

More broadly, these findings suggest that aspects of dosing error risk are encoded in upstream trial design and protocol characteristics, reinforcing the value of preventive, design-stage interventions for improving medication safety in clinical research. By enabling early identification of trials that warrant closer scrutiny, the proposed approach supports a proactive shift from reactive error detection toward anticipatory risk management.

4.2 Limitations and future directions

This study has a few limitations that warrant consideration. First, dosing error labels were derived from adverse event reports in ClinicalTrials.gov and may therefore be affected by underreporting. Nevertheless, the use of a large-scale dataset drawn from a single, standardized reporting system provides a consistent basis for comparative analysis across a heterogeneous population of CTs, supporting the identification of trial-level risk patterns within the scope of the available data.

Second, although a multimodal modeling strategy was adopted, the integration of structured and unstructured information was implemented using a deliberately simple late-fusion approach. More sophisticated multimodal architectures may warrant further investigation and could potentially yield additional performance gains. However, the improvements observed with this basic fusion strategy suggest that the different data modalities capture complementary risk-related information, indicating that multimodal integration remains beneficial even under conservative modeling assumptions.

Third, while full protocol documents were collected and converted into machine-readable text, the present study did not exploit this source of information. Such documents often contain detailed dosing procedures and other relevant clinical details but pose substantial methodological challenges due to their length, heterogeneity, and complex structure.

Although addressing these challenges represents an exciting direction for future research, it was beyond the scope of the present study. In this context, the dataset and processing pipeline introduced here provide a foundation for further investigation. The dataset has additionally been released as part of the CT-DEB 2026 shared task, hosted within the CL4Health workshop at LREC 2026, to stimulate further research on protocol-level document analysis for CT safety.

5 Conclusion

In this study, we introduced an ML framework for early, trial-level stratification of dosing error risk in CTs. By enabling straightforward adaptation to other categories of medication errors, alternative definitions of acceptable error rate thresholds, and different CT inclusion criteria, the proposed framework can be readily tailored to specific regulatory, operational, or safety objectives. The approach leverages information available prior to trial initiation to support proactive risk assessment at the planning stage. Experimental results demonstrate that the framework can stratify CTs according to dosing error risk using pre-initiation information. Importantly, the observed frequency of trials exhibiting high dosing error rates within each predicted risk group was aligned with the predefined probability bounds used to define these categories, supporting the reliability of the resulting risk stratification. Moreover, the preservation of risk trends across development phases and enrollment categories further supports the structural robustness of the proposed stratification framework.

This study highlights two key methodological insights. First, multimodal integration of structured trial information and unstructured protocol text consistently improved trial-level discrimination performance, even when implemented using a deliberately simple late-fusion strategy, underscoring the complementary nature of these data sources. Second, probability calibration appeared to be critical for aligning predicted risks with interpretable probability thresholds, enabling reliable and flexible risk stratification beyond binary classification. From a practical perspective, the proposed framework supports early, trial-level risk assessment that may inform proactive quality management in clinical research. By providing interpretable risk categories prior to trial initiation, the approach may support the identification of trials that warrant additional review, protocol refinement, or targeted quality safeguards.

A key strength of the proposed framework lies in its reproducibility, scalability, and interpretability. All components of the pipeline, from data extraction and label construction to model training and evaluation, are publicly released and rely exclusively on publicly available data sources, enabling straightforward regeneration of the dataset under alternative inclusion criteria or temporal cut-offs and facilitating reuse across a broad range of research activities related to CT safety. This infrastructure provides a foundation for future methodological extensions, including the exploration of more sophisticated multimodal architectures and the exploitation of full protocol documents. Ultimately, early, data-driven trial-level risk assessment represents a promising direction for supporting improvements in the safety and quality of clinical research.

Author contributions

Félicien Hêche: Conceptualization; Methodology; Investigation; Formal analysis; Writing – original draft; **Sohrab Ferdowsi:** Conceptualization; Methodology; Data curation; Investigation; Writing – review & editing. **Anthony Yazdani:** Methodology; Data curation; Writing – review & editing. **Sara Sansaloni-Pastor:** Writing – review & editing. **Douglas Teodoro:** Conceptualization; Supervision; Funding acquisition; Writing – review & editing.

Funding statement

This work was supported by Innosuisse – the Swiss Innovation Agency – grant number 114.721 IP-ICT

Conflict of interest

Sara Sansaloni-Pastor works for Actelion Pharmaceuticals Ltd. The other authors declare no competing interests.

Data availability

All source data were obtained from the publicly accessible ClinicalTrials.gov registry. The curated dataset generated in this study is publicly available on Hugging Face. The full analysis pipeline and model implementation are available on GitHub.

References

- [1] Jeffrey K Aronson. Medication errors: definitions and classification. *British journal of clinical pharmacology*, 67(6):599–604, 2009.
- [2] Rachel Ann Elliott, Elizabeth Camacho, Dina Jankovic, Mark J Sculpher, and Rita Faria. Economic analysis of the prevalence and clinical and economic burden of medication error in england. *BMJ Quality & Safety*, 30(2):96–105, 2021.
- [3] Mahsa Rouhani, Maryam Mousavi, Mohammad Mahdi Kooshyar, Soodabeh Shahidsales, Yasha Makhdoumi, Amir Amirabadi, and Sepideh Elyasi. Application of a chemotherapy standard form in patients with breast cancer: comparison of private and public centers. *Jundishapur Journal of Natural Pharmaceutical Products*, 13(3), 2018.
- [4] Alexander Hodkinson, Natasha Tyler, Darren M Ashcroft, Richard N Keers, Kanza Khan, Denham Phipps, Aseel Abuzour, Peter Bower, Anthony Avery, Stephen Campbell, et al. Preventable medication harm across health care settings: a systematic review and meta-analysis. *BMC medicine*, 18:1–13, 2020.
- [5] WHO Global Patient Safety Challenge. Medication without harm. *World Health Organization*, 2017. <https://www.who.int/initiatives/medication-without-harm> [Accessed: (11 April 2025)].
- [6] World Health Organization. *Medication without harm: policy brief*. World Health Organization, 2024. <https://www.who.int/publications/i/item/9789240062764>[Accessed: (11 April 2025)].
- [7] Dinggang Shen, Guorong Wu, and Heung-II Suk. Deep learning in medical image analysis. *Annual review of biomedical engineering*, 19(1):221–248, 2017.
- [8] Alessandro Carriero, Léon Groenhoff, Elizaveta Vologina, Paola Basile, and Marco Albera. Deep learning in breast cancer imaging: State of the art and recent advancements in early 2024. *Diagnostics*, 14(8):848, 2024.
- [9] Aditi Govindu and Sushila Palwe. Early detection of parkinson’s disease using machine learning. *Procedia Computer Science*, 218:249–261, 2023.
- [10] Wongeun Song, Se Young Jung, Hyunyoung Baek, Chang Won Choi, Young Hwa Jung, Sooyoung Yoo, et al. A predictive model based on machine learning for the early detection of late-onset neonatal sepsis: development and observational study. *JMIR medical informatics*, 8(7):e15965, 2020.
- [11] Dimitris Bertsimas, Agni Orfanoudaki, and Rory B Weiner. Personalized treatment for coronary artery disease patients: a machine learning approach. *Health care management science*, 23(4):482–506, 2020.
- [12] Xiaoqing Tan, Chung-Chou H Chang, Ling Zhou, and Lu Tang. A tree-based model averaging approach for personalized treatment effect estimation from heterogeneous data sources. In *International Conference on Machine Learning*, pages 21013–21036. PMLR, 2022.
- [13] Douglas Teodoro, Nona Naderi, Anthony Yazdani, Boya Zhang, and Alban Bornet. A scoping review of artificial intelligence applications in clinical trial risk assessment. *medRxiv*, pages 2025–01, 2025.
- [14] Sohrab Ferdowsi, Julien Knafou, Nikolay Borissov, David Vicente Alvarez, Rahul Mishra, Poorya Amini, and Douglas Teodoro. Deep learning-based risk prediction for interventional clinical trials based on protocol design: A retrospective study. *Patterns*, 4(3), 2023.
- [15] Sohrab Ferdowsi, Nikolay Borissov, Julien Knafou, Poorya Amini, and Douglas Teodoro. Classification of hierarchical text using geometric deep learning: the case of clinical trials corpus. *arXiv preprint arXiv:2110.15710*, 2021.
- [16] Julián N Acosta, Guido J Falcone, Pranav Rajpurkar, and Eric J Topol. Multimodal biomedical ai. *Nature medicine*, 28(9):1773–1784, 2022.
- [17] Elisa Warner, Joonsang Lee, William Hsu, Tanveer Syeda-Mahmood, Charles E Kahn Jr, Olivier Gevaert, and Arvind Rao. Multimodal machine learning in image-based and clinical biomedicine: Survey and prospects. *International Journal of Computer Vision*, 132(9):3753–3769, 2024.
- [18] Vitor Cerqueira, Luis Torgo, and Carlos Soares. A case study comparing machine learning with statistical methods for time series forecasting: size matters. *Journal of Intelligent Information Systems*, 59(2):415–433, 2022.
- [19] Anthony Yazdani, Alban Bornet, Philipp Khlebnikov, Boya Zhang, Hossein Rouhizadeh, Poorya Amini, and Douglas Teodoro. An evaluation benchmark for adverse drug event prediction from clinical trial results. *Scientific Data*, 12(1):424, 2025.
- [20] Eric J Topol. High-performance medicine: the convergence of human and artificial intelligence. *Nature medicine*, 25(1):44–56, 2019.

- [21] Geir Thore Berge, Ole-Christoffer Granmo, Tor Oddbjørn Tveit, Bjørn Erik Munkvold, Anna Linda Ruthjersen, and Jivitesh Sharma. Machine learning-driven clinical decision support system for concept-based searching: a field trial in a norwegian hospital. *BMC Medical Informatics and Decision Making*, 23(1):5, 2023.
- [22] Félicien Hêche, Sohrab Ferdowsi, Anthony Yazdani, et al. Machine learning for medication error detection: A scoping review. *Research Square*, February 2026. Research Square preprint, Version 1. Available at: <https://doi.org/10.21203/rs.3.rs-8919709/v1>.
- [23] Amitabh Chandra, John Drum, Michael Daly, Henry Mirsberger, Samuel Spare, Ulrich Neumann, Silas Martin, and Noam Kirson. Comprehensive measurement of biopharmaceutical r&d investment. *Nat Rev Drug Discov*, 23:652–653, 2024.
- [24] Bernard Vrijens, Antoine Pironet, and Eric Tousset. The importance of assessing drug exposure and medication adherence in evaluating investigational medications: ensuring validity and reliability of clinical trial results. *Pharmaceutical Medicine*, 38(1):9–18, 2024.
- [25] Rayhan A. Tariq, Rishik Vashisht, Ankur Sinha, and Yevgeniya Scherbak. *Medication Dispensing Errors and Prevention*. StatPearls Publishing, Treasure Island (FL), 2025.
- [26] European Medicines Agency. Guideline for the notification of serious breaches of regulation (eu) no 536/2014 or the clinical trial protocol. https://www.ema.europa.eu/en/documents/scientific-guideline/guideline-notification-serious-breaches-regulation-eu-no-5362014-or-clinical-trial-protocol_en.pdf, 2023. Accessed: 2025-09-09.
- [27] Chi Heem Wong, Kien Wei Siah, and Andrew W Lo. Estimation of clinical trial success rates and related parameters. *Biostatistics*, 20(2):273–286, 01 2018.
- [28] Linda Martin, Melissa Hutchens, and Conrad Hawkins. Trial watch: clinical trial cycle times continue to increase despite industry efforts. *Nature Reviews Drug Discovery*, 16(3):157–158, 2017.
- [29] Aylin Sertkaya, Hui-Hsing Wong, Amber Jessup, and Trinidad Beleche. Key cost drivers of pharmaceutical clinical trials in the united states. *Clinical Trials*, 13(2):117–126, 2016.
- [30] Pydantic AI. Data validation using python type hints. <https://github.com/pydantic/pydantic>.
- [31] Python Software Foundation. enum — support for enumerations. <https://docs.python.org/3/library/enum.html>. Accessed: 2026-01-07.
- [32] MedDRA. Medical dictionary for regulatory activities (meddra), 2025. Accessed: 2025-09-12.
- [33] Paul Beninger. Signal management in pharmacovigilance: a review of activities and case studies. *Clinical therapeutics*, 42(6):1110–1129, 2020.
- [34] Tianqi Chen. Xgboost: A scalable tree boosting system. *Cornell University*, 2016.
- [35] Simon A Lee, Anthony Wu, and Jeffrey N Chiang. Clinical modernbert: An efficient and long context encoder for biomedical text. *arXiv preprint arXiv:2504.03964*, 2025.
- [36] W Brier Glenn et al. Verification of forecasts expressed in terms of probability. *Monthly weather review*, 78(1):1–3, 1950.
- [37] Chuan Guo, Geoff Pleiss, Yu Sun, and Kilian Q Weinberger. On calibration of modern neural networks. In *International conference on machine learning*, pages 1321–1330. PMLR, 2017.
- [38] Ben Van Calster, David J McLernon, Maarten Van Smeden, Laure Wynants, and Ewout W Steyerberg. Calibration: the achilles heel of predictive analytics. *BMC medicine*, 17(1):230, 2019.
- [39] John Platt et al. Probabilistic outputs for support vector machines and comparisons to regularized likelihood methods. *Advances in large margin classifiers*, 10(3):61–74, 1999.
- [40] Bianca Zadrozny and Charles Elkan. Transforming classifier scores into accurate multiclass probability estimates. In *Proceedings of the eighth ACM SIGKDD international conference on Knowledge discovery and data mining*, pages 694–699, 2002.
- [41] PyMuPDF Developers. Pymupdf documentation. <https://pymupdf.readthedocs.io/en/latest/>, 2025. Accessed: 2026-01-07.
- [42] Haoran Wei, Yaofeng Sun, and Yukun Li. Deepseek-ocr: Contexts optical compression. *arXiv preprint arXiv:2510.18234*, 2025.
- [43] Takuya Akiba, Shotaro Sano, Toshihiko Yanase, Takeru Ohta, and Masanori Koyama. Optuna: A next-generation hyperparameter optimization framework. In *Proceedings of the 25th ACM SIGKDD international conference on knowledge discovery & data mining*, pages 2623–2631, 2019.

A Categorical features encoding

This appendix describes the encoding of some of the categorical structured features extracted from ClinicalTrials.gov. Each feature was mapped to predefined integer identifiers representing distinct categories, ensuring consistent and interpretable model inputs. The resulting mappings are reported in Table 5.

Feature	ID	Meaning
phases	0	NA (not reported)
	1	EARLY_PHASE1
	2	PHASE1
	3	PHASE2
	4	PHASE3
	5	PHASE4
primaryPurpose	0	TREATMENT
	1	PREVENTION
	2	DIAGNOSTIC
	3	ECT
	4	SUPPORTIVE_CARE
	5	SCREENING
	6	HEALTH_SERVICES_RESEARCH
	7	BASIC_SCIENCE
	8	DEVICE_FEASIBILITY
	9	OTHER
masking	0	NONE
	1	SINGLE
	2	DOUBLE
	3	TRIPLE
	4	QUADRUPLE
sex	0	ALL
	1	FEMALE
	2	MALE
armGroupTypes	0	EXPERIMENTAL
	1	ACTIVE_COMPARATOR
	2	PLACEBO_COMPARATOR
	3	SHAM_COMPARATOR
	4	NO_INTERVENTION
	5	OTHER
interventionTypes	0	DRUG
	1	DEVICE
	2	BIOLOGICAL
	3	PROCEDURE
	4	RADIATION
	5	BEHAVIORAL
	6	GENETIC
	7	DIETARY_SUPPLEMENT
	8	COMBINATION_PRODUCT
	9	DIAGNOSTIC_TEST
	10	OTHER

Table 5: Overview of mappings between categorical features and their corresponding integer encodings. For multi-label variables, multiple category identifiers may be associated with a single trial.

B Additional extracted information

This appendix describes the auxiliary information extracted in parallel with the features and labels used in the present study. These variables were not incorporated into the primary modeling framework but were curated to facilitate regeneration of the dataset under alternative inclusion criteria or labeling strategies, and enable secondary analyses related to CT safety and design characteristics. A complete overview of these elements is provided in Table 6. In addition to fields directly available from ClinicalTrials.gov, full trial protocols, typically provided as lengthy PDF documents, were also downloaded and extracted from the links provided within the trials. These downloaded PDF documents were then converted into machine-readable text using PyMuPDF [41]. The accompanying codebase further supports optical character recognition-based extraction via DeepSeek-OCR [42] for more careful serialization.

Name	Data type / encoding	Description
overallStatus	Categorical	Overall recruitment status of the trial
leadSponsorClass	Categorical	Sponsor class
hasProtocol	Binary indicator	Indicates whether a protocol document is available
hasSap	Binary indicator	Indicates whether a statistical analysis plan document is available
hasIcf	Binary indicator	Indicates whether an informed consent form document is available
startDate	Date	Trial initiation date
completionDate	Date	Trial completion date
nctId	String	ClinicalTrials.gov unique trial identifier (NCT number)
leadSponsorName	String	Name of the lead sponsor organization
protocolPdfLinks	String	Links to protocol PDF document(s) when available
protocolPdfText	String	Machine-readable text extracted from available trial protocol PDF document(s)
count_X	Numeric (count)	Family of variables capturing the number of adverse event reports mapped to MedDRA dosing-error term X
wilson_lower_bound	Numeric (continuous)	Lower bound of the 95% Wilson confidence interval for the dosing error rate
ct_level_ade_population	Numeric (count)	Number of participants at risk of experiencing an adverse drug event
sum_dosing_errors	Numeric (count)	Number of dosing errors
dosing_error_rate	Numeric (continuous)	Number of dosing errors normalized by the number of patients at risk

Table 6: Overview of additional information extracted.

C Implementation details

Hyperparameters of the XGBoost model were optimized using Optuna [43], with the search space summarized in Table 7. A total of 200 hyperparameter configurations were evaluated, and the model achieving the best AUC-ROC score on the validation set was selected for final evaluation on the test set. To address class imbalance, positive samples were upweighted via a class-weighting parameter, which was jointly optimized during hyperparameter tuning. Missing values in structured features were managed using XGBoost’s native missing-value mechanism.

The ClinicalModernBERT model was trained with a maximum context length of 8,192 tokens, a learning rate of 2.5×10^{-5} , a weight decay of 0.01, and an effective batch size of 32 achieved through gradient accumulation over four steps. Hyperparameters were not tuned but selected based on prior experience with this architecture. Training was conducted for up to 100 epochs, with early stopping applied using a patience of five epochs. To mitigate class imbalance, class-balanced mini-batch sampling was employed, enforcing a fixed proportion of 0.5 positive samples per batch. For text fields with missing values, empty entries were replaced with a dedicated string (“UNKNOWN”) prior to tokenization.

For the LateFusion model, the fusion weight used to combine the unimodal predicted probabilities was selected to maximize the AUC-ROC score on the validation set using Optuna over 100 trials.

Hyperparameter	Search range	Description
n_estimators	100 – 1000	Number of boosting trees
max_depth	3 – 12	Maximum depth of individual decision trees
learning_rate	$[10^{-3}, 0.3]$	Learning rate controlling the contribution of each tree; sampled on a logarithmic scale
subsample	0.5 – 1.0	Fraction of training samples randomly subsampled for each tree
colsample_bytree	0.5 – 1.0	Fraction of features randomly subsampled for each tree
gamma	0 – 5	Minimum loss reduction required to make a further partition on a leaf node
min_child_weight	1 – 10	Minimum sum of instance weights required in a child node
max_delta_step	0 – 10	Maximum change in leaf weights allowed per boosting iteration
reg_alpha	$[10^{-8}, 10]$	L1 regularization strength on model weights; sampled on a logarithmic scale
reg_lambda	$[10^{-8}, 10]$	L2 regularization strength on model weights; sampled on a logarithmic scale
scale_pos_weight	$[0.5w, 2.0w]$	Class imbalance weighting, where w denotes the empirical ratio of negative to positive samples

Table 7: XGBoost hyperparameter search space.

D Additional results

This appendix reports the risk stratification results for all evaluated ML models on the test set. Table 8 summarizes the distribution of CTs across predefined risk groups for both calibrated and uncalibrated model variants.

	Number of CTs	Number of events	Event rate (%)	Relative risk
XGBoost (uncal.)				
Low	79	0	0.00	0.000
Moderate	1311	1	0.08	0.015
High	1252	8	0.64	0.130
Very high	3676	301	8.19	1.669
XGBoost				
Low	3422	22	0.64	0.131
Moderate	896	24	2.68	0.546
High	975	79	8.10	1.651
Very high	1025	185	18.05	3.68
ClinicalModernBERT (uncal.)				
Low	4002	33	0.83	0.168
Moderate	391	17	4.35	0.886
High	253	10	3.95	0.806
Very high	1672	250	14.95	3.047
ClinicalModernBERT				
Low	3741	24	0.64	0.131
Moderate	853	33	3.87	0.788
High	520	41	7.88	1.607
Very high	1204	212	17.61	3.589

Table 8: Risk stratification results for all evaluated models on the test set. Results are shown for both calibrated and uncalibrated variants using predefined risk group cut-offs applied consistently across models.

E Risk stratification by enrollment size

This appendix reports the results of the risk stratification analysis according to trial enrollment size. Table 9 summarizes the distribution of CTs across predefined risk categories within each enrollment bin (≤ 50 , 51–200, 201–500, and >500 participants) on the test set. For each category, we report the number of trials, the number of problematic trials, the observed event rate, and the relative risk computed with respect to the baseline prevalence within the corresponding enrollment group.

Risk group	Number of CTs	Number of events	Event rate (%)	Relative risk
Enrollment ≤ 50				
Low	2535	16	0.63	0.517
Moderate	328	5	1.52	1.248
High	124	8	6.45	5.283
Very high	43	8	18.60	15.236
Enrollment 51–200				
Low	912	4	0.44	0.099
Moderate	421	13	3.09	0.698
High	354	32	9.04	2.042
Very high	301	39	12.96	2.927
Enrollment 201–500				
Low	92	2	2.17	0.198
Moderate	149	8	5.37	0.488
High	191	13	6.81	0.619
Very high	332	61	18.37	1.671
Enrollment > 500				
Low	8	0	0.00	0.000
Moderate	50	0	0.00	0.000
High	69	5	7.25	0.385
Very high	409	96	23.47	1.246

Table 9: Risk stratification by enrollment size on the test set using calibrated LateFusion predictions. Relative risks are reported with respect to the baseline prevalence within each enrollment group.